Reaction $^{52}Cr(p,\gamma)^{53}Mn$ from 1.66 to 2.91 MeV

G. U. Din,* I. A. Al-Agil, and A. M. A. Al-Soraya
Van de Graaff Laboratory, King Saud University, Riyadh, Saudi Arabia

J. A. Cameron
Department of Physics, McMaster University, Hamilton, Ontario, Canada L8S 4K1
(Received 15 April 1991)

The resonant proton capture reaction $^{52}Cr(p,\gamma)^{53}Mn$ has been observed in the proton energy range 1.66 to 2.91 MeV ($8.19 < E_x < 9.42$ MeV), with a resolution of 2.5 keV FWHM. Altogether 192 resonance peaks were found, many of which were multiplets. Gamma-ray spectra and angular distributions were used to fix or limit spins for 82 of the resonances, among which are analogs of four ^{53}Cr states from 1.29 to 2.32 MeV.

I. INTRODUCTION

The level structure of ^{53}Mn ($N=28$) is adequately described within the framework of the shell model. It has been shown [1] that the inclusion of a single proton excitation into the pf shell provides a good representation of the levels up to 2.5 MeV. Above this, the higher level density observed requires further excitations. Only above 7 MeV do analogs of ^{53}Cr states appear [2]. Studies of the lowest three analogs and those of some higher ^{53}Cr levels, including the $g_{9/2}$ state, have been reported [3–11]. The excitation energy region from 8 to 9 MeV contains the expected location of a number of $l=3$ analogs. The first of these, a $\frac{5}{2}^-$ state at 8.05 MeV, corresponding to the 1.006-MeV level of ^{53}Cr, was examined in some detail and a number of fragments were found [7]. This analog state had previously been seen in $(^3He,d)$ proton-stripping measurements [8]. The analog of the $\frac{7}{2}^-$ intruder state at 1.537 MeV in ^{53}Cr, with its rather small (d,p) spectroscopic factor, was also reported in Ref. [8], although the analog of the stronger 1.290-MeV $\frac{7}{2}^-$ state was not. A further $\frac{5}{2}^-$ level at 1.974 MeV in ^{53}Cr is seen only weakly in the (d,p) reaction and no analog has been identified. The high energy limit of the present search range includes the 9.29-MeV multiplet identified [5,8–10] as the analog of the $\frac{3}{2}^-$ 2.321-MeV level of ^{53}Cr. The $(^3He,d)$ experiments [8] also revealed two $l=4$ levels in ^{53}Mn at lower energy than the $g_{9/2}$ analog resonance but well above the expected position of the antianalog, as yet unidentified. The lower of these "orphan" states was observed also as a (p,γ) doublet and its spin assignment confirmed, but the higher one was not seen [12].

Previous to the (p,γ) work of Ref. [7], there were three broad surveys of resonances in the $^{52}Cr+p$ system, both with high resolution. The (p,γ) yield curve of Vuister [13] extends in proton energy from 1.37 into 2.26 MeV, while the elastic-scattering experiment by Moses *et al.* [9] is from 2.1 to 3.2 MeV and that of Wylie *et al.* [10] is from 2.4 to 4.1 MeV. Vuister did not measure angular distributions and spectra were taken with scintillation counters, so no J^π values are available. The elastic-scattering yields of $l=3$ states at such low energies are too small for reliable determinations of the total angular momentum J.

II. EXPERIMENT

The experiments were carried out at the AK Van de Graaff of King Saud University and the KN Van de Graaff accelerator at McMaster University. The methods employed followed the pattern established in earlier (p,γ) surveys [7,14–16]. An extensive yield curve was measured in steps of about 1 keV, using a 10-$\mu g/cm^2$ target of enriched ^{52}Cr on a high-purity tungsten backing. Gamma rays were observed at 55° using a HPGe detector and the yields in the γ energy ranges 7.0–9.5 and 2.0–5.0 MeV were compared. These represent, respectively, capture to the lowest two states of ^{53}Mn ($\frac{7}{2}^-$ and $\frac{5}{2}^-$) and secondaries from capture to higher states. At the stronger resonances spectra were collected and, in a number of cases, angular distributions were measured. In this case, a detector 10 cm from the target was rotated through five angles (0°, 30°, 45°, 60°, and 90°) and a second HPGe detector was placed close to the target (at −90°) in order to monitor and compensate for small beam energy and intensity variations. Standard methods of analysis were used to obtain angular-distribution coefficients and to search for appropriate spin parameters. At the higher energies, inelastic scattering becomes strong, and the angular distribution of the 1.434-MeV $2^+ \rightarrow 0^+$ ^{52}Cr γ ray was used as well.

Several of the resonances are evidently broadened. In these cases, spectra were collected in small proton energy intervals and yield curves were constructed for each of the strong γ-decay channels.

III. RESULTS

A. Excitation functions

Figure 1 and Table I show the almost 200 resonance peaks found in the 1.25-MeV energy range surveyed, from 1.66- to 2.91-MeV proton energy. The system reso-

lution of about 2.5 keV FWHM (including both target thickness and beam-energy broadening) implies that about one-third of the observed peaks are likely to be unresolved multiplets. This is confirmed by comparing the present results with those of Vuister [13] in the region of overlap, up to 2.26 MeV. After allowing for the difference in resolution, the agreement between Fig. 1 and Fig. 3 of Ref. [13] is excellent. The beam-energy calibration was confirmed by deducing the resonant excitation energies from the γ-ray spectra. The internal consistency of these was generally about 1 keV and their calibration using the impurity lines of $^{19}F(p,\alpha)^{16}O$ (6.130 MeV) and $^{23}Na(p,\alpha)^{20}Ne$ (1.632 MeV) had equivalent precision. The proton beam energy was thence derived using the Q value of 6.561(1) MeV [2].

During long exposures for the collection of γ spectra

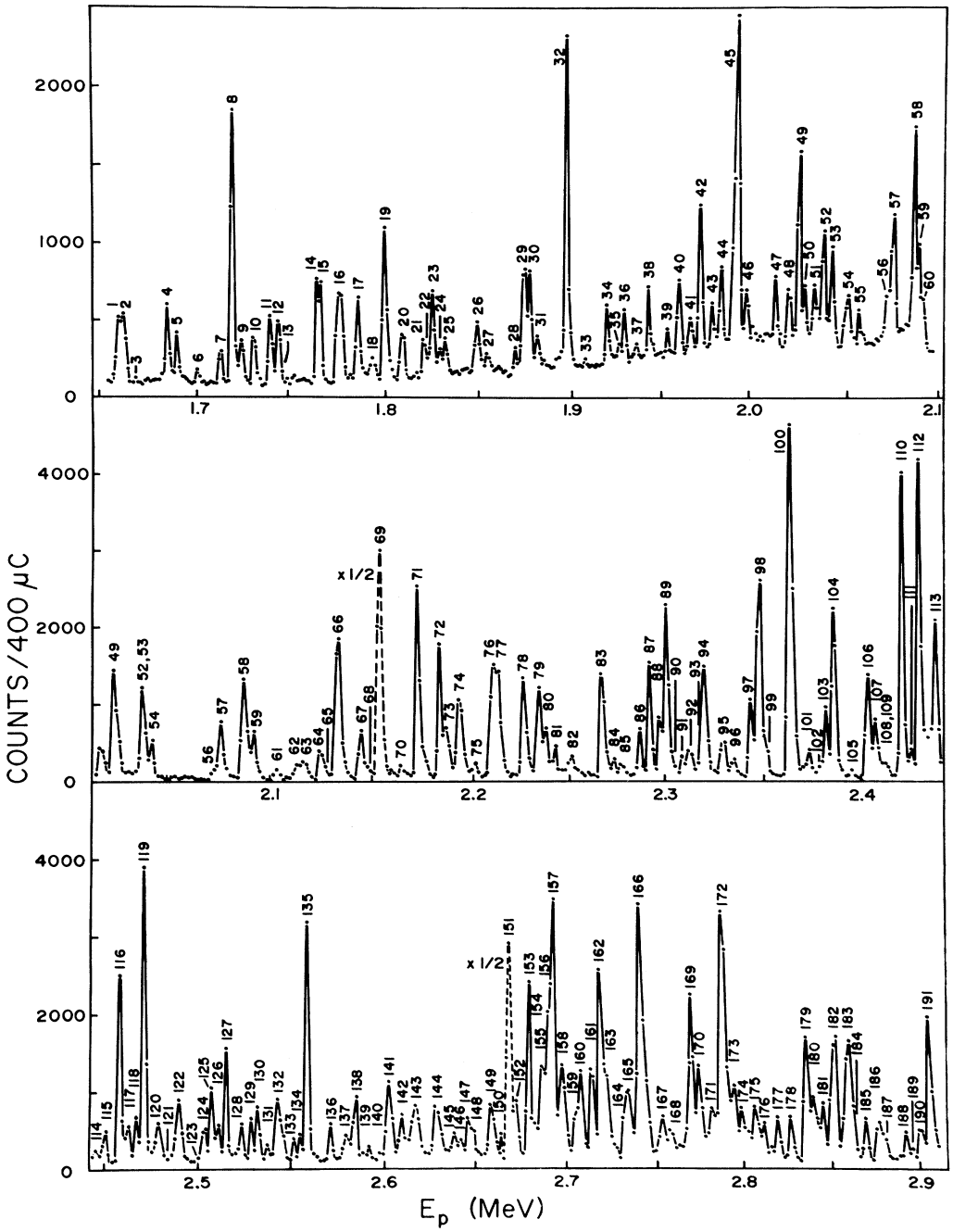

FIG. 1. Yield of the $^{53}Cr(p,\gamma)$ reaction in the proton energy range $1.65 < E_p < 2.92$ MeV with $7 < E_\gamma < 9$ MeV. The top sector from 1.65 to 2.10 MeV was measured at King Saud University, the remainder, including some overlap, at McMaster University.

TABLE I. Resonances in $^{52}Cr(p,\gamma)^{53}Mn$ from 1.66 to 2.91 MeV.

Res. no.	E_p (MeV)	E_x (MeV)	J^π
1	1.660	8.189	
2	1.663	8.192	
3	1.669	8.198	
4	1.686	8.215	
5	1.691	8.220	
6	1.702	8.230	
7	1.713	8.242	
8	1.720	8.248	$\frac{3}{2}^-, \frac{5}{2}^-$
9	1.725	8.254	
10	1.732	8.260	
11	1.740	8.268	$(\frac{3}{2}^-, \frac{5}{2}^-)$
12	1.744	8.272	
13	1.747	8.275	
14	1.764	8.292	$(\frac{3}{2}^-, \frac{5}{2}^-)$
15	1.767	8.294	$(\frac{3}{2}^-, \frac{5}{2}^-)$
16	1.776	8.304	$\frac{5}{2}^-$
17	1.786	8.313	
18	1.794	8.321	
19	1.800	8.327	$\frac{5}{2}^-, \frac{7}{2}^-$
20	1.810	8.336	$\frac{3}{2}^-$
21	1.821	8.348	
22	1.823	8.350	
23	1.826	8.352	
24	1.830	8.356	
25	1.832	8.359	
26	1.849	8.376	
27	1.855	8.381	
28	1.870	8.396	
29	1.875	8.400	$(\frac{3}{2}^-, \frac{5}{2}^-)$
30	1.878	8.404	$\frac{3}{2}^-$
31	1.882	8.407	
32	1.896	8.422	$\frac{3}{2}^-$
33	1.909	8.434	
34	1.919	8.444	
35	1.927	8.452	
36	1.930	8.454	$\frac{5}{2}^{(+)}$
37	1.936	8.460	
38	1.943	8.468	
39	1.954	8.478	
40	1.960	8.484	$\frac{3}{2}^{(-)}$
41	1.966	8.490	
42	1.971	8.495	$\frac{5}{2}, \frac{7}{2}^{(-)}$
43	1.978	8.502	$(\frac{3}{2}^-, \frac{5}{2}^-)$
44	1.983	8.507	$(\frac{3}{2}^-, \frac{5}{2}, \frac{7}{2}^-)$
45*A*	1.991	8.515	$\frac{3}{2}^-, \frac{5}{2}^-$
45*B*	1.993	8.516	$\frac{7}{2}^-$
46	1.997	8.520	
47	2.013	8.536	
48	2.017	8.540	
49	2.023	8.456	$(\frac{1}{2}-\frac{5}{2}$ and $\frac{7}{2}^-, \frac{9}{2}^+)$
50	2.026	8.549	
51	2.034	8.557	
52	2.037	8.560	$(\frac{3}{2}^-, \frac{5}{2}^-)$
53	2.042	8.565	$(\frac{3}{2}^-, \frac{5}{2}, \frac{7}{2}^-)$
54	2.052	8.575	
55	2.058	8.580	
56	2.072	8.594	
57	2.075	8.597	
58	2.087	8.609	$(\frac{3}{2}^-, \frac{5}{2}^-)$
59	2.088	8.610	
60	2.091	8.613	$(\frac{3}{2}^-, \frac{5}{2}, \frac{7}{2}^-)$
61	2.103	8.624	
62	2.112	8.633	
63	2.117	8.638	
64	2.124	8.645	
65	2.128	8.649	
66	2.133	8.654	$(\frac{3}{2}^-)$
67	2.144	8.665	
68	2.149	8.670	
69	2.154	8.674	$(\frac{3}{2}^-)$
70	2.164	8.684	
71	2.172	8.692	$(\frac{3}{2}^-, \frac{5}{2}, \frac{7}{2}^-)$
72	2.184	8.703	
73	2.187	8.707	
74	2.194	8.714	$(\frac{3}{2}^-, \frac{5}{2}, \frac{7}{2})$
75	2.201	8.721	
76	2.210	8.729	
77	2.213	8.732	$\frac{5}{2}^-$
78	2.226	8.745	$(\frac{3}{2}^-, \frac{5}{2}, \frac{7}{2}^-)$
79	2.235	8.754	
80	2.238	8.756	
81	2.243	8.762	
82	2.251	8.769	
83	2.267	8.785	$(\frac{3}{2}^-, \frac{5}{2}\frac{7}{2}^-)$
84	2.273	8.791	
85	2.279	8.797	
86	2.286	8.804	
87	2.291	8.809	$(\frac{3}{2}^-, \frac{5}{2}, \frac{7}{2}^-)$
88	2.296	8.814	
89	2.300	8.817	$\frac{5}{2}$
90	2.305	8.822	
91	2.308	8.826	
92	2.311	8.829	

TABLE I. (*Continued*).

Res. no.	E_p (MeV)	E_x (MeV)	J^π
93	2.318	8.835	
94	2.321	8.838	$\frac{5}{2}$
95	2.329	8.846	$(\frac{3}{2}^-,\frac{5}{2}^+)$
96	2.335	8.852	
97	2.344	8.860	$(\frac{3}{2}^-,\frac{5}{2}^+)$
98	2.348	8.865	$\frac{5}{2}$
99	2.352	8.869	
100	2.364	8.881	$\frac{5}{2}$
101	2.374	8.890	
102	2.379	8.895	
103	2.383	8.899	
104	2.386	8.902	$(\frac{3}{2}^-,\frac{5}{2},\frac{7}{2}^-)$
105	2.397	8.913	
106	2.404	8.920	$(\frac{3}{2}^-,\frac{5}{2}^+)$
107	2.407	8.922	$(\frac{3}{2}^-,\frac{5}{2},\frac{7}{2}^-)$
108	2.409	8.924	$\frac{7}{2}^-$
109	2.410	8.925	$\frac{5}{2}^-,\frac{7}{2}^-$
110	2.422	8.937	$\frac{5}{2}^-$
111	2.427	8.943	
112	2.431	8.946	$\frac{5}{2},\frac{7}{2}^-$
113	2.439	8.954	$(\frac{5}{2}^-,\frac{7}{2}^-)$
114	2.446	8.961	
115	2.452	8.967	
116	2.459	8.973	$(\frac{3}{2}^-,\frac{5}{2},\frac{7}{2}^-)$
117	2.464	8.978	$(\frac{3}{2}^-,\frac{5}{2},\frac{7}{2}^-)$
118	2.468	8.981	$(\frac{3}{2}^-,\frac{5}{2},\frac{7}{2})$
119	2.472	8.985	
120	2.480	8.994	$\frac{3}{2}^-,\frac{5}{2}$
121	2.483	8.997	$(\frac{5}{2}^-,\frac{7}{2})$
122	2.490	9.004	$(\frac{3}{2}^-,\frac{5}{2},\frac{7}{2}^-)$
123	2.499	9.013	
124	2.503	9.017	
125	2.508	9.021	
126	2.511	9.025	
127	2.515	9.028	$(\frac{3}{2}^-,\frac{5}{2},\frac{7}{2}^-)$
128	2.523	9.037	
129	2.529	9.042	
130	2.532	9.045	
131	2.538	9.051	
132	2.541	9.054	
133	2.552	9.064	
134	2.555	9.068	
135	2.559	9.071	$\frac{3}{2}^{(-)}$
136	2.571	9.084	
137	2.580	9.092	
138	2.585	9.098	$(\frac{3}{2}^-,\frac{5}{2}^-)$
139	2.589	9.101	
140	2.597	9.109	
141	2.604	9.115	$(\frac{3}{2}^-,\frac{5}{2},\frac{7}{2}^-)$
142	2.610	9.122	$(\frac{3}{2}^-,\frac{5}{2}^-)$
143	2.617	9.129	
144	2.629	9.140	$(\frac{3}{2}^-,\frac{5}{2}^+)$
145	2.639	9.150	
146	2.643	9.154	$(\frac{3}{2}^-,\frac{5}{2}^+)$
147	2.646	9.157	
148	2.650	9.161	
149	2.659	9.170	$(\frac{3}{2}^-,\frac{5}{2},\frac{7}{2}^-)$
150	2.664	9.175	
151	2.670	9.180	$\frac{5}{2}^-$
152	2.673	9.184	
153	2.681	9.191	$\frac{5}{2}$
154	2.684	9.195	$\frac{9}{2}^+$
155	2.688	9.198	$(\frac{3}{2}^-,\frac{5}{2},\frac{7}{2}^-)$
156	2.691	9.202	$(\frac{3}{2}^-,\frac{5}{2},\frac{7}{2}^-)$
157	2.695	9.205	$\frac{9}{2}^+$
158	2.699	9.209	$\frac{5}{2}^-$
159	2.706	9.216	
160	2.710	9.219	$\frac{3}{2}^-,\frac{5}{2}^-,\frac{7}{2}^-$
161	2.716	9.226	$(\frac{3}{2}^-,\frac{5}{2},\frac{7}{2}^-)$
162	2.721	9.230	$\frac{5}{2}^-$
163	2.724	9.234	
164	2.733	9.243	$(\frac{3}{2}^-,\frac{5}{2},\frac{7}{2}^-)$
165	2.737	9.246	$(\frac{3}{2}^-,\frac{5}{2}^-)$
166	2.742	9.252	$\frac{5}{2}$
167	2.755	9.264	
168	2.760	9.269	
169	2.770	9.279	$\frac{5}{2}^-$
170	2.776	9.284	$\frac{3}{2}^-$
171	2.783	9.291	
172	2.789	9.297	$\frac{3}{2}^-$
173	2.796	9.304	$\frac{3}{2},\frac{5}{2}^-$
174	2.800	9.308	$\frac{7}{2}^-$
175	2.807	9.315	$\frac{5}{2}^-$
176	2.812	9.320	$\frac{3}{2}^-$
177	2.820	9.328	
178	2.826	9.333	
179	2.837	9.344	$\frac{3}{2}^-$
180	2.840	9.348	$(\frac{3}{2}^-,\frac{5}{2},\frac{7}{2}^-)$
181	2.846	9.353	
182	2.855	9.362	$(\frac{3}{2}^-,\frac{5}{2},\frac{7}{2}^-)$
183	2.859	9.366	

TABLE I. (*Continued*).

Res. no.	E_p (MeV)	E_x (MeV)	J^π	Res. no.	E_p (MeV)	E_x (MeV)	J^π
184	2.865	9.372		189	2.898	9.404	
185	2.872	9.379		190	2.901	9.408	
186	2.875	9.382		191	2.906	9.412	
187	2.883	9.389		192	2.911	9.417	$(\frac{3}{2}^-)$
188	2.894	9.400					

and angular distributions, beam-energy stability was monitored using the count rate in the broad energy ranges used for the yield curves. This generally remained constant relative to the beam current to about 10%, implying a stability of about 0.5 keV over the exposure time.

There is a systematic discrepancy of about 4 keV between the excitation energies of Table I and those of Ref. [13]. It is difficult to compare the present yield curves with those measured for elastic scattering. Moses *et al.* [9] report no $l=3$ resonance but do identify many $l=1,2$ resonances against which Table I may be compared. The present proton energies appear to be within 1 keV of those measured by the Duke group [9], who made an absolute calibration using the ^{7}Li(p,n) threshold.

B. Resonance decay schemes

From the γ-ray spectra at resonances, using the known efficiencies of the detectors used, decay branching to bound states of ^{53}Mn was deduced. This is shown in Table II for 79 resonances. It is important to recognize that the spectra in many cases contain cross contamina-

TABLE II. Decay branching from ^{52}Cr$(p,\gamma)^{53}$Mn resonances.

Res. no.	8	11	14	15	16	19	20	29	30	32	36	40	42	43	44	45[a]
0.0	5				71	9		8	4	1	16		79		20	58
0.378	75	47	3	2	16	46	19	67	20	56	15	16		7		10
1.290	2		18	51	2	4	17	13	32	6		6		5		8
1.441																
1.621																
2.274	1		19	7		10				22		5		7	39	2
2.407	1	14				18			4			4	2		5	1
2.573	2				1	9							6			2
2.671		6		4			10	2	11			4				4
2.686		24	19	7			6	5	6	1		3		16		4
2.707				2			5		6		23			1	3	
2.876	11				2		6		3	1		3		4	3	1
2.913	1	9	9	6			13			1		2	1			
3.007			2	3			4		3		46	3		2		1
3.097				1			7					9				2
3.102						4				2			6	2	10	
3.127					3					1						1
3.182			6		1					1		3			3	2
3.200												2				
3.381															6	1
3.466					1		7			1						
3.480			18	11												
3.532					1		2			2		2		7		
3.666							4			1		3		6		
3.850															3	
3.898			3	3				5	7	2		18		12		
3.955	1												1		1	
3.960												2				
3.999															2	
4.062					1											1
4.066				1					2	1		2	5	7		1
4.083																

TABLE II. (*Continued*).

Res. no.	8	11	14	15	16	19	20	29	30	32	36	40	42	43	44	45[a]
4.240															2	
4.266				2								4			3	
4.300												6		6		
4.348			3						2					4		
4.428	1															1
4.552										1		2				
4.719												6				
4.780														1		
4.793														3		
4.955														10		

Res. no.	49	52	53	58	60	66	69	71	74	77	78	83	87	89	94	95
0.0	76	35	16	5	7	67	62	73	86	50	11	7	3	80	49	5
0.378	3	27	20	63	40		7	19	14	5	64	58	49	13	47	8
1.290	4	11	10	7	38		13			25	8		8		4	8
1.441	7															
1.621																
2.274		4		6	6	13	4					8	7			2
2.407		2	6	4	4	5	4			14	3		3			39
2.573		13	7			3						3	13	2		4
2.671				5			2									
2.686			11	1								5				3
2.707						3	2									2
2.876		1	8	2									2			2
2.913												3				
3.007	1		7			1		1				1				
3.097							2	2				1				
3.102	4			3												3
3.127		1	4	1							5			3		3
3.182		2	3			2				3		9		2		10
3.200						1		2		1						5
3.381	2		3													
3.466	1										2					
3.480				2		2	1									
3.532		1										2				
3.666						1						1				
3.850																
3.898		2				1	1									
3.955																
3.960											4					3
3.999			3													2
4.062			2								3					
4.066	1			1	3	1	1			1		1				1
4.083																
4.240																
4.266								1								
4.300	1															
4.348							1	1								
4.428								1								
4.552																
4.719																
4.780		1										1				
4.793					2					1						
4.955	10															

TABLE II. (*Continued*).

Res. no.	97	98	100	104	106[b]	107[b]	108[b]	109[b]	110	112	113	116	117	118	120	121
0.0	17	77	53	14	28	48	9	3	47	8	23	39	10	6	27	59
0.378	43	3	20	51	13	6	27	26	29	85	37	42	70	74	73	15
1.290		5	15	10	12			7			3					
1.441							4									
1.621							4				7					11
2.274	9		1		4	6	7			2	1			1		
2.407	9	4	1	5	3	3	8	7	3	2	7	7				
2.573		1							2		1	3				
2.671									2							
2.686				4	27	19	7	3	9	2		3		10		
2.707	6	1			3											
2.876	7	2	1		6	11		6			1					
2.913								11								
3.007		2		5	1		5	18	2		3		8			
3.097		3	1	3						1				1		
3.102	3										2			1		
3.127							6	4						1		
3.182			5				2				2		12	1		
3.200	3						13				5					
3.381			3		3	7	8		2		2	4				
3.466											1	2		2		
3.480																
3.532				4					1		1			1		
3.666								8	2							
3.850																
3.898																
3.955																8
3.960								7								
3.999																
4.062																
4.066	3	1		4										2		
4.083																
4.240																
4.266									1		2					7
4.300																
4.348																
4.428		1									2					
4.552																
4.719																
4.780																
4.793																
4.955																

Res. no.	122	127	135	138	141	142	144	146	149	151	153	154[c]	155[c]	156[c]	157[c]	158
0.0	22	2	1	23	13	3	31	12	1	8	33	61	21	27	59	36
0.378	17	68	71	1	16	23	17	14	9	51	10	6	43	60	3	39
1.290	5	5	9	19	22	4	14	31	43	14		10	17	3	10	4
1.441												12			3	
1.621																
2.274	19		2	3	4	4	8								6	7
2.407			3	10	8		10	15	12				9		4	
2.573					4	4				3	7			2		
2.671			4			5										9
2.686			2	8	7	16	4					4				
2.707			3				2	13								
2.876		9	2	3	3	8						7				5
2.913					5	4				3						

TABLE II. (*Continued*).

Res. no.	122	127	135	138	141	142	144	146	149	151	153	154[c]	155[c]	156[c]	157[c]	158
3.007		6	3	10					9		14		5		5	
3.097	6				1			12		5					3	
3.102				7		10					4			1		
3.127	4	2				4				2	6					
3.182				3	7	9	4		10	5	13		5		2	
3.200	7	3								6				2	3	
3.381	3						5							1		
3.466	8			2	3					1						
3.480																
3.532	5			2						2						
3.666				4	3											
3.850																
3.898				2				3						1	2	
3.955																
3.960				2												
3.999									7					1		
4.062																
4.066		2		1		2					13			2		
4.083						4	5									
4.240																
4.266					4											
4.300																
4.348	4								6							
4.438		3							3							
4.552																
4.719																
4.780																
4.793																
4.955																

Res. no.	160	161	162	164	165	166	169	170	172	174	175	179	180	182	192
0.0	22	21	20	5	4	53	12	3	4	29	5	5	5	32	2
0.378	19	48	37	55	34	10	17	30	80	10	95	10	7	40	7
1.290	8	14	4	10	13	14	31	12		9		6	39		33
1.441										7					
1.621															
2.274	7		5	11	12		3	4	3				5	9	4
2.407	9	3	9			2	11	11		5		11	18	8	5
2.573			2				4							4	2
2.671		3				1	2	8							6
2.686		4	5				1	17		8		6	2		2
2.707								2				4			1
2.876	17	3			5	2	2	3		9		23			5
2.913	8					2				16					3
3.007				5		6	3	1				21			3
3.097			1		5		4		1			5	7	3	
3.102															
3.127			3				3	9	2	7		4			3
3.182			2	7	8	2	2							2	
3.200					4	2			2				7	1	
3.381			2	7									7		4
3.466		2	2				1		2						4
3.480			2				2					5			
3.532	7		1												4
3.666			1										3	1	
3.850															
3.898					7	1	2								

TABLE II. (*Continued*).

Res. no.	160	161	162	164	165	166	169	170	172	174	175	179	180	182	192
3.955	3														
3.960															2
3.999															
4.062		2	2												4
4.066						2			1						4
4.083						2									
4.240															
4.266			1						1						2
4.300									1						
4.348				3											
4.428			1	4		1			1						1
4.552															
4.719															
4.780															
4.793									1						
4.955				1					1						

[a]Doublet, see Fig. 2.
[b]Multiplet, see Fig. 3.
[c]Multiplet, see Ref. [9].

tion from neighboring resonances. Accordingly, although the strong branches are likely reliable to a precision of a few percent, weak branches may be highly uncertain, unless it is seen that they are absent in the neighbors. Care was, of course, taken to ensure consistent sums of Dopper-corrected primary γ-ray energy and final-state excitation energy, but, especially in the case of weak branches, this is limited to about 2-keV uncertainty.

C. Close resonances

In many instances, close-lying resonances lead to discernible broadening of the peaks in the yield curve. The careful comparison of the yields in different wide γ windows sometimes showed a small shift in centroid position indicating different preferences for decay from unresolved components. This led in an early scan [12] to the discovery of a pair of previously unknown $\frac{9}{2}^+$ resonances at 2.7 MeV. Two further instances are given here at 2.0 and 2.4 MeV.

Figures 2(a) and (b) show yield curves taken carefully, in 600-eV steps, near $E_p = 2.0$ MeV. In the main peak, there are evidently two components (resonances 45 *A* and *B*) whose different decay modes are made evident in the single branch yields of Figs. 2(c)–(h). The peak separation is about 1.2 keV.

Figure 3 shows a similar scan around 2.4 MeV. In this case there appear to be two clear peaks, centered at 2.405 and 2.409 MeV. In the yield curves to single final states, however, four resonances appear (106–109).

D. Angular distributions and J^π assignments

It is seldom possible to make a unique spin assignment on the basis of a single capture γ angular distribution.

TABLE III. Bound-state spins in ^{53}Mn.

E_x (MeV)	J^π [a]	E_x (MeV)	J^π [a]	E_x (MeV)	J^π [a]
0.0	$\frac{7}{2}^-$	2.671	$\frac{1}{2}^-$	3.480	$\frac{1}{2}^-$
0.378	$\frac{5}{2}^-$	2.686	$\frac{7}{2}^-$	3.666	$\frac{5}{2}^-$
1.290	$\frac{3}{2}^-$	2.707	$\frac{1}{2}^+$	3.898	$\frac{1}{2}^-$
1.441	$\frac{11}{2}^-$	2.876	$\frac{3}{2}^-$	3.955	$\frac{7}{2}^-$ [b]
1.621	$\frac{9}{2}^-$	2.913	$\frac{3}{2}^-$	4.066	$\frac{3}{2}^-$
2.274	$\frac{5}{2}^-$	3.097	$\frac{3}{2}^-$	4.428	$\frac{3}{2}^-$
2.407	$\frac{3}{2}^-$	3.127	$\frac{5}{2}^-$	4.719	$\frac{1}{2}^-$
2.573	$\frac{7}{2}^-$	3.182	$\frac{3}{2}^-$ [b]	3.955	$\frac{1}{2}^-$

[a]Reference [2], except as noted.
[b]Reference [7].

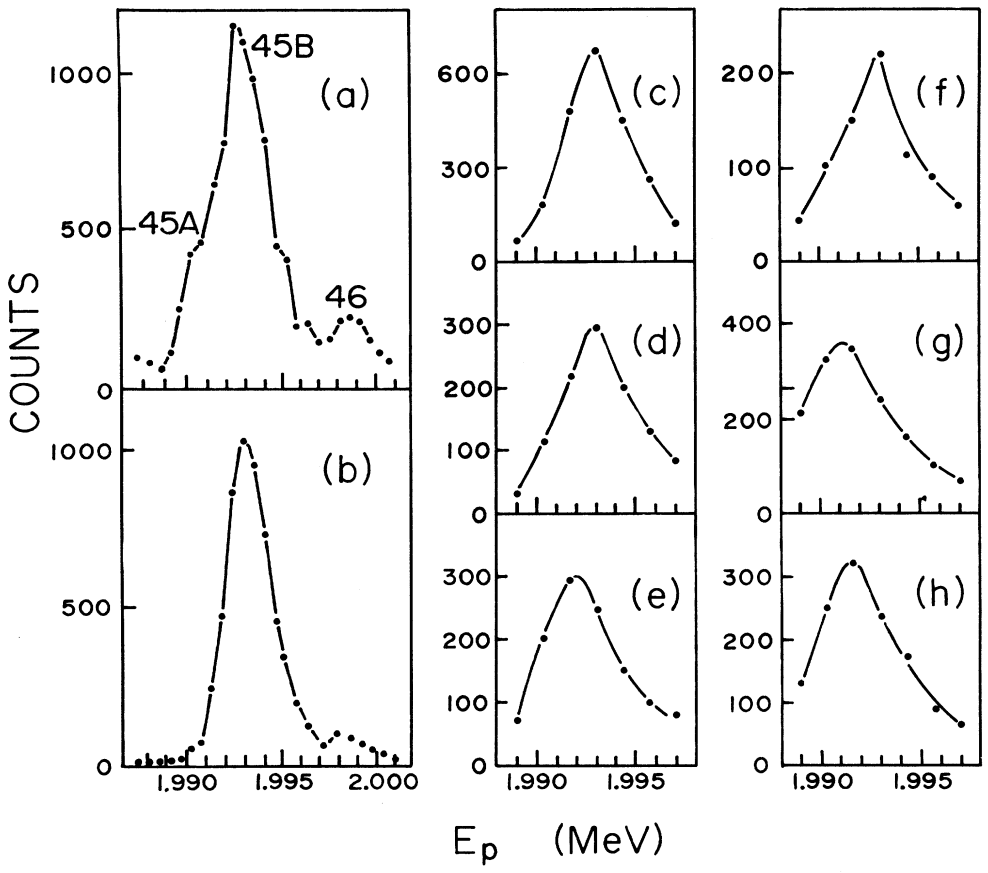

FIG. 2. Single-channel yield curves near $E_p = 2.0$ MeV. (a) $2 < E_\gamma < 5$ MeV, (b) $E_\gamma > 7$ MeV. Primary transitions to final states at (c) 0.0, (d) 0.378, (e) 1.290, (f) 2.686, (g) 3.182, (h) 4.062 MeV.

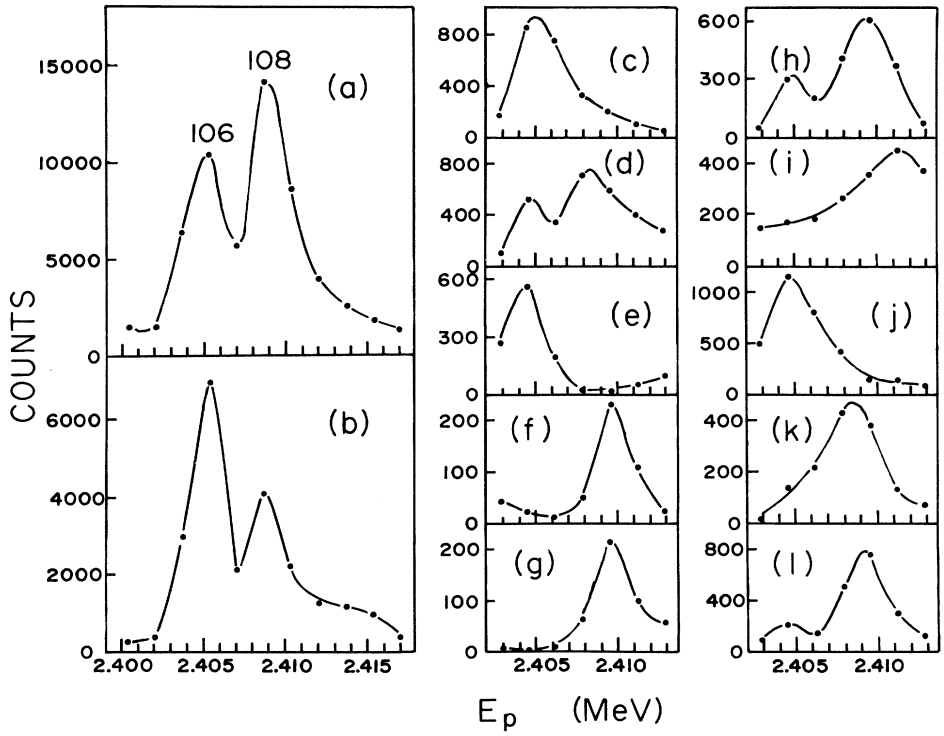

FIG. 3. Single-channel yield curves near $E_p = 2.4$ MeV. (a) $2 < E_\gamma < 5$ MeV, (b) $E_\gamma > 7$ MeV. Primary transitions to final states at (c) 0.0, (d) 0.378, (e) 1.290, (f) 1.441, (g) 1.621, (h) 2.274, (i) 2.407, (j) 2.686, (k) 3.129, (l) 3.198 MeV.

TABLE IV. Angular distributions.

Res. no.	E_i (MeV)	E_f (MeV)	J_f^π	A_2	A_4	J_i^π
8	8.248	0.0	$\frac{7}{2}^-$	0.09(9)	0.02(10)	
		0.378	$\frac{5}{2}^-$	0.38(3)	0.17(3)	$\frac{3}{2}^-, \frac{5}{2}^-$
		2.876	$\frac{3}{2}^-$	−0.44(4)	0.07(4)	
16	8.304	0.0	$\frac{7}{2}^-$	−0.15(3)	0.05(4)	$\frac{5}{2}^-$
		0.378	$\frac{5}{2}^-$	0.17(3)	0.08(6)	
19	8.327	0.0	$\frac{7}{2}^-$	0.08(11)	0.26(12)	
		0.378	$\frac{5}{2}^-$	0.34(4)	0.17(4)	
		2.274	$\frac{5}{2}^-$	0.40(7)	−0.04(7)	$\frac{5}{2}^-, \frac{7}{2}^-$
		2.573	$\frac{7}{2}^-$	−0.26(6)	0.01(6)	
20	8.336	2.913	$\frac{3}{2}^-$	−0.45(5)	0.13(6)	$\frac{3}{2}^-, \frac{5}{2}^-$
30	8.404	0.378	$\frac{5}{2}^-$	0.20(4)	0.04(4)	
		1.290	$\frac{3}{2}^-$	−0.33(7)	0.09(8)	$\frac{3}{2}^-$
		2.672	$\frac{1}{2}^-$	−0.60(9)	0.26(10)	
32	8.422	0.378	$\frac{5}{2}^-$	0.24(3)	0.08(3)	$\frac{3}{2}^-, \frac{7}{2}^-$
		2.274	$\frac{5}{2}^-$	−0.29(3)	0.11(3)	
36	8.454	3.007	$\frac{5}{2}^+$	0.59(6)	−0.12(6)	$\frac{3}{2}^+, \frac{5}{2}, \frac{7}{2}^+, \frac{9}{2}^+$
40	8.484	0.378	$\frac{5}{2}^-$	−0.14(5)	0.06(5)	
		3.097	$\frac{3}{2}^-$	0.37(8)	0.05(8)	$\frac{3}{2}$
		3.898	$\frac{1}{2}^-$	−0.71(5)	0.03(5)	
42	8.495	0.0	$\frac{7}{2}^-$	−0.24(3)	0.05(3)	$\frac{5}{2}, \frac{7}{2}$
45*A*	8.515	1.290	$\frac{3}{2}^-$	−0.11(7)	0.28(7)	$\frac{3}{2}^-, \frac{5}{2}^-$
45*B*	8.516	0.0	$\frac{7}{2}^-$	−0.17(3)	0.07(3)	$\frac{5}{2}^-$
		0.378	$\frac{5}{2}^-$	0.31(6)	0.10(6)	
77	8.732	0.0	$\frac{7}{2}^-$	−0.20(3)	0.01(3)	
		1.290	$\frac{3}{2}^-$	−0.44(3)	0.01(3)	$\frac{5}{2}^-$
		2.407	$\frac{3}{2}^-$	−0.12(4)	0.03(4)	
89	8.817	0.0	$\frac{7}{2}^-$	−0.20(3)	0.05(3)	$\frac{5}{2}$
94	8.838	0.0	$\frac{7}{2}^-$	−0.20(3)	0.06(3)	$\frac{5}{2}$
		0.378	$\frac{5}{2}^-$	0.38(4)	0.13(4)	
98	8.865	0.0	$\frac{7}{2}^-$	−0.24(4)	0.12(4)	$\frac{5}{2}, \frac{9}{2}$
100	8.881	0.0	$\frac{7}{2}^-$	−0.22(4)	0.08(4)	
		0.378	$\frac{5}{2}^-$	0.35(5)	0.17(5)	$\frac{5}{2}$
		1.290	$\frac{3}{2}^-$	−0.51(5)	0.01(5)	
108	8.924	0.0	$\frac{7}{2}^-$	0.16(7)	0.09(8)	
		0.378	$\frac{5}{2}^-$	−0.15(4)	0.15(5)	$\frac{5}{2}^-, \frac{7}{2}^-$
		1.621	$\frac{9}{2}^-$	0.50(19)	−0.02(2)	
		2.686	$\frac{7}{2}^-$	0.00(7)	0.21(7)	
109	8.925	0.0	$\frac{7}{2}^-$	−0.16(8)	−0.04(8)	$\frac{5}{2}^-, \frac{7}{2}^-$
		0.378	$\frac{5}{2}^-$	−0.01(4)	−0.05(5)	
110	8.937	0.0	$\frac{7}{2}^-$	−0.19(4)	0.11(4)	
		0.378	$\frac{5}{2}^-$	0.29(5)	0.19(6)	$\frac{5}{2}^-$
		2.407	$\frac{3}{2}^-$	0.06(8)	0.01(9)	
		2.686	$\frac{7}{2}^-$	0.09(6)	0.16(6)	
112	8.946	0.0	$\frac{7}{2}^-$	−0.15(7)	0.22(8)	$\frac{5}{2}, \frac{7}{2}^-$
		0.378	$\frac{5}{2}^-$	0.40(4)	0.14(4)	

TABLE IV. (*Continued*).

Res. no.	E_i (MeV)	E_f (MeV)	J_f^π	A_2	A_4	J_i^π
119	8.994	0.0	$\frac{7}{2}^-$	−0.18(4)	0.08(4)	$\frac{5}{2}, \frac{7}{2}^-$
		0.378	$\frac{5}{2}^-$	0.41(5)	0.24(5)	
134	9.071	0.378	$\frac{5}{2}^-$	−0.17(3)	0.10(3)	$\frac{3}{2}, \frac{7}{2}^-$
		1.290	$\frac{3}{2}^-$	0.44(9)	0.14(9)	
151	9.180	0.0	$\frac{7}{2}^-$	−0.18(9)	−0.07(9)	
		0.378	$\frac{5}{2}^-$	0.63(7)	−0.11(8)	$\frac{5}{2}^-$
		1.290	$\frac{3}{2}^-$	−0.21(4)	−0.14(4)	
		inel.		0.51(4)	−0.32(4)	
153	9.191	0.0	$\frac{7}{2}^-$	−0.09(3)	−0.10(3)	$\frac{5}{2}$
		1.290	$\frac{3}{2}^-$	−0.29(3)	−0.12(3)	
154	9.195	0.0	$\frac{7}{2}^-$	−0.29(4)	−0.08(4)	
		1.441	$\frac{11}{2}^-$	−0.25(4)	−0.07(4)	$\frac{9}{2}$
		2.686	$\frac{7}{2}^-$	−0.29(6)	−0.08(6)	
157	9.205	0.0	$\frac{7}{2}^-$	−0.50(4)	0.10(4)	$\frac{9}{2}$
		1.441	$\frac{11}{2}^-$	−0.27(6)	0.15(6)	
158	9.209	0.0	$\frac{7}{2}^-$	−0.04(4)	−0.16(5)	
		0.378	$\frac{5}{2}^-$	0.50(4)	−0.04(5)	$\frac{5}{2}^-, \frac{7}{2}^-$
		1.290	$\frac{3}{2}^-$	0.51(9)	−0.28(10)	
		inel.		0.34(4)	0.17(5)	
160	9.219	0.0	$\frac{7}{2}^-$	0.31(9)	0.07(10)	$\frac{3}{2}^-, \frac{5}{2}^-, \frac{7}{2}^-$
		0.378	$\frac{5}{2}^-$	0.20(9)	0.17(10)	
162	9.230	0.0	$\frac{7}{2}^-$	0.47(5)	−0.21(5)	
		0.378	$\frac{5}{2}^-$	0.31(4)	−0.17(4)	
		2.407	$\frac{3}{2}^-$	0.37(4)	−0.11(4)	$\frac{5}{2}^-$
		2.686	$\frac{7}{2}^-$	0.26(5)	−0.23(6)	
		inel.		0.60(3)	−0.50(3)	
166	9.252	0.0	$\frac{7}{2}^-$	−0.17(3)	−0.09(3)	
		0.378	$\frac{5}{2}^-$	0.50(9)	−0.05(9)	$\frac{5}{2}$
		1.290	$\frac{3}{2}^-$	−0.28(4)	−0.00(5)	
		inel.		0.57(2)	−0.16(2)	
169	9.279	0.0	$\frac{7}{2}^-$	−0.04(6)	0.03(6)	
		0.378	$\frac{5}{2}^-$	0.21(5)	0.02(5)	
		1.290	$\frac{3}{2}^-$	0.22(4)	−0.14(4)	$\frac{5}{2}^-$
		2.407	$\frac{3}{2}^-$	−0.32(6)	0.02(5)	
		inel.		0.39(2)	−0.16(2)	
170	9.284	0.378	$\frac{5}{2}^-$	−0.01(7)	0.12(7)	$\frac{1}{2}^-, \frac{3}{2}^-$
		inel.		0.03(2)	0.09(2)	
172	9.297	0.378	$\frac{5}{2}^-$	−0.28(3)	0.04(4)	$\frac{3}{2}^-, \frac{7}{2}^-$
		inel.		0.30(3)	0.15(3)	
173	9.304	0.0	$\frac{7}{2}^-$	0.01(8)	−0.22(8)	$\frac{3}{2}^-, \frac{5}{2}^-$
		inel.		0.44(4)	0.12(5)	
174	9.308	0.0	$\frac{7}{2}^-$	−0.12(4)	−0.20(4)	
		0.378	$\frac{5}{2}^-$	−0.11(8)	−0.08(8)	$\frac{7}{2}^-$
		1.290	$\frac{3}{2}^-$	0.41(8)	−0.24(8)	
175	9.315	0.0	$\frac{7}{2}^-$	0.25(14)	−0.20(14)	
		0.378	$\frac{5}{2}^-$	−0.10(3)	−0.13(3)	$\frac{5}{2}^-$
		inel.		0.58(5)	−0.13(5)	
176	9.326	inel.		0.15(4)	0.07(4)	$\frac{3}{2}^-$
178	9.340	inel.		0.15(4)	0.05(5)	$\frac{3}{2}^-$

TABLE V. Comparison of (^{3}He,d) and (p,γ) results.

Ref. [8]				Present work	
E_x (MeV)	l	J^π	Res. no.	E_x (MeV)	J^π
8.188	1		1	8.189	
			2	8.192	
8.421	1		32	8.422	$\frac{3}{2}^-$
8.516	3		45A	8.515	$\frac{3}{2}^-, \frac{5}{2}^-$
			45B	8.516	$\frac{7}{2}^-$
8.883	2(3)	$\frac{5}{2}^{(+)}$	100	8.881	$\frac{5}{2}$
8.982	2(3)	$\frac{5}{2}^{(+)}$	117	8.978	$(\frac{3}{2}^-, \frac{5}{2}^-, \frac{7}{2}^-)$
			118	8.981	$(\frac{3}{2}^-, \frac{5}{2}, \frac{7}{2}^-)$
9.106	2	$\frac{5}{2}^{(+)}$	140	9.109	
9.194	4		154	9.195	$\frac{9}{2}^+$
9.248	2	$\frac{5}{2}^+$	166	9.252	$\frac{5}{2}$
9.282	1	$\frac{3}{2}^-$	170	9.284	$\frac{3}{2}^-$

Therefore, at the strong capture resonances, angular distributions of several decay branches were analyzed wherever possible. Of the 42 bound states populated in this study, the spins and parities of 24, shown in Table III, are established [2,7]. The present results are shown in Table IV. In many cases the decay branches observed in the capture spectra were used to place limits on the spins and parities of resonances, assuming only dipole and electric quadrupole transitions to be strongly competitive. Where no angular distributions were available, the assignments in Table I are shown in parentheses. In a few cases, the spectra were used to reduce ambiguities from angular-distribution measurements.

IV. DISCUSSION

A. Resonances, J^π values

The correlation of present results for the energies, spins, and parities of proton resonances with earlier work is good. Identification of the resonances of Table I with those of Vuister [13] and of Moses *et al.* [9] depends largely on the spacing pattern, since the former did not deduce J^π values and the latter elastic-scattering experiment is sensitive in this energy range only to resonances with $l<3$. Only two of the $l=2$ J assignments in Ref. [9] are incompatible with the present results.

Four (p,γ) resonances studied by Maripuu [3] fall in the energy range of the present experiment. They are identified with resonances 8, 11, 14 and 15, and 19 of Table I. In all cases the spin assignments are compatible, though those of Ref. [3] are more restrictive.

The (p,γ) yield curve of Kleinwächter *et al.* from 2.73 to 2.81 MeV (Ref. [5], Fig. 2) is similar to the corresponding part of Fig. 1, resonances 164–175. Our spin assignments of $\frac{3}{2}^-$ to resonances 170 and 172 agree with those assumed in Ref. [5] by identification with the strong $\frac{3}{2}^-$ elastic-scattering resonances [9,10].

Although many proton-stripping experiments to ^{53}Mn have been performed, only that of Galès *et al.* [8] extends into the excitation energy region studied here. Fourteen stripping peaks (21–34 in Table I of Ref. [8]) lie in the region 8.18–9.42 MeV. Of these, nine are assigned l values and, in five cases, J^π values from d-p angular correlations. Corresponding resonances are to be found in the present work, as indicated in Table V.

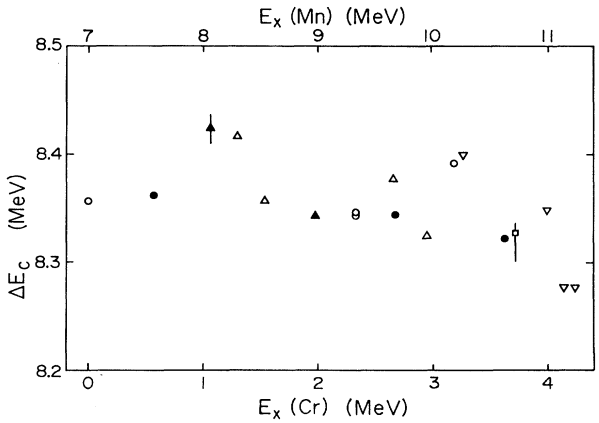

FIG. 4. Variation of the Coulomb displacement energy with excitation energy for $A=53$: ● ($\frac{1}{2}^-$), ○ ($\frac{3}{2}^-$), ▽ ($\frac{5}{2}^+$), ▲ ($\frac{5}{2}^-$), △ ($\frac{7}{2}^-$), □ ($\frac{9}{2}^+$). The vertical bars represent the width of multiplets.

B. Isobaric analog states

The present analog state assignments, and those of others, up to 4.2 MeV in ^{53}Cr, are summarized in Table VI and Fig. 4. The excitation energy region in ^{53}Mn spanned by the present work, from 8.19 to 9.42 MeV, corresponds to the energy range in the isobaric parent nucleus ^{53}Cr $1.15 < E_x < 2.38$ MeV which contains three $l=3$ levels at 1.290 ($\frac{7}{2}^-$), 1.537 ($\frac{7}{2}^-$), and 1.974 MeV ($\frac{5}{2}^-$) and a ($\frac{3}{2}^-$) level at 2.321 Mev. In addition, states of high spin exist at 2.172 and 2.233 MeV. The analog of the Cr 2.321-MeV level was identified in (^{3}He,d) [8] and resonant proton scattering [9,10] as a group of levels around 9.29 MeV. The present results add little to the conclusions previously draw [8–10,5] about this analog multiplet but confirm the identification of the two strongest fragments chosen by Kleinwächter *et al.* [5]. A number of weaker $\frac{3}{2}^-$ resonances may also be fragments of the analog state.

Galès *et al.* identified their $l=3$ stripping peak at 8.516 MeV as the analog of the 1.537-MeV Cr level, then thought to have spin $\frac{5}{2}$, but since found to be $\frac{7}{2}^-$. The main component (B) of resonance 45 has $J^\pi = \frac{7}{2}^-$ and is therefore taken to be the analog state. Until this work, no analog of the 1.290-MeV state had been found. Reso-

TABLE VI. Isobaric analogs in $A=53$. M denotes the centroid of fragmented analog.

^{53}Cr			^{53}Mn		
E_x (MeV)	J^π	Res. no.	E_x (MeV)	J^π	ΔE_C (MeV)
0.0	$\frac{3}{2}^-$		6.977	$\frac{3}{2}^-$	8.357[a]
0.564	$\frac{1}{2}^-$		7.546	$\frac{1}{2}^-$	8.362[a,b]
1.006	$\frac{5}{2}^-$		8.050 (M)	$\frac{5}{2}^-$	8.424[a,c]
1.290	$\frac{7}{2}^-$	19	8.327	$\frac{5}{2}^-, \frac{7}{2}^-$	8.417
		42	8.495	$\frac{5}{2}, \frac{7}{2}^{(-)}$	8.336
1.537	$\frac{7}{2}^-$	44	8.507	$(\frac{3}{2}^-, \frac{5}{2}, \frac{7}{2}^-)$	8.348
		45B	8.516	$\frac{7}{2}^-$	8.357[a]
		110	8.937	$\frac{5}{2}^-$	8.343
1.974	$\frac{5}{2}^-$	112	8.946	$\frac{5}{2}, \frac{7}{2}^-$	8.352
		113	8.954	$(\frac{5}{2}^-, \frac{7}{2}^-)$	8.360
2.321	$\frac{3}{2}^-$	170	9.284	$\frac{3}{2}^-$	8.343[a,d,e,g]
		172	9.297	$\frac{3}{2}^-$	8.346[d,g]
2.657	$(\frac{5}{2}, \frac{7}{2})^-$		9.656	$\frac{5}{2}^-, \frac{7}{2}^-$	8.379[a,g]
2.671	$\frac{1}{2}^-$		9.636	$\frac{1}{2}^-$	8.345[d]
2.993	$(\frac{5}{2}, \frac{7}{2})^-$		9.938	$(\frac{5}{2}, \frac{7}{2})^-$	8.325[a]
3.180	$(\frac{3}{2})^-$		10.175	$\frac{3}{2}^-$	8.375[f,g]
3.262	$(\frac{5}{2})^+$		10.285 (M)	$\frac{5}{2}^+$	8.403[f]
3.617	$\frac{1}{2}^-$		10.558	$\frac{1}{2}^-$	8.321[a,f,g]
3.707	$\frac{9}{2}^+$		10.662 (M)	$\frac{9}{2}^+$	8.335[a,h,i]
3.985	$(\frac{5}{2})^+$		10.955	$\frac{5}{2}^+$	8.350[f]
4.135	$(\frac{3}{2}, \frac{5}{2})^+$		11.033	$\frac{3}{2}^+, \frac{5}{2}^+$	8.278[f,g]
4.231	$(\frac{3}{2}, \frac{5}{2})^+$		11.125	$\frac{3}{2}^+, \frac{5}{2}^+$	8.274[g]

[a]Reference [8].
[b]Reference [3].
[c]Reference [7].
[d]Reference [11].
[e]Reference [12].
[f]Reference [13].
[g]Reference [5].
[h]Reference [4].
[i]Reference [6].

nance 19 appears to be the only $\frac{7}{2}^-$ candidate available. However, Maripuu [3] assigns a spin of $\frac{5}{2}$ to this resonance. Neither of the two low-lying $\frac{7}{2}^-$ states of ^{53}Cr has a large stripping strength. The lower level is generally regarded as being a multiparticle excitation within the fp shell, the higher one a particle-hole excitation from the $f_{7/2}$ shell. Accordingly, it is not surprising that their analogs have resisted discovery and that their relative capture strengths to low-lying states of ^{53}Mn, largely of $f_{7/2}$ character, are about 2:1 in favor of the higher state, compared to the reverse for neutron stripping to the Cr parents.

The 1.974-MeV $\frac{5}{2}^-$ level of ^{53}Cr is only weakly populated in the (d,p) reaction. Resonances 100, 112, and 113, near 8.94 MeV in ^{53}Mn are proposed as fragments of its analog, spread over about 20 keV, as is the lower $\frac{5}{2}^-$ analog at 8.05 MeV [7].

Higher analogs proposed by others are included in Table VI and Fig. 4. The decrease in the Coulomb displacement energy near 4 MeV is similar to that found in other nuclei [14–16] and results from spreading of the wave function of the quasibound protons as the top of the Coulomb barrier is approached. The discontinuities apparent in the lowest 3 MeV are more difficult to interpret. The difference in the two $\frac{7}{2}^-$ states suggest that an explanation might be found in terms of the occupancy of the $f_{7/2}$ shell, rather than the l dependence suggested in Ref. [5]. At such high excitation, l values are usually strongly mixed, as the small spectroscopic factors attest.

V. CONCLUSIONS

The present work, together with Ref. [7], provides a continuous (p,γ) survey of ^{53}Mn levels from 7.9 to 9.4 MeV. Detailed decay branching and angular-distribution measurements have led to spin assignments. Wherever connection has been possible with the results of other experiments, particularly $(^3\text{He},d)$ and resonant elastic proton scattering, good agreement has been found. Three $l=3$ isobaric analog states are reported here for the first time in capture.

The authors wish to acknowledge the help of operations staff at both the King Saud AK and McMaster KN accelerators, and the financial support of the Research Centre of King Saud University and of the National Sciences and Engineering Research Council of Canada.

*Deceased.

[1] B. C. Metsch and P. W. M. Glaudemans, Nucl. Phys. **A352**, 60 (1981).
[2] L. K. Peker, Nucl. Data Sheets **43**, 481 (1984); Huo Junde and Hu Dailing, *ibid.* **61**, 47 (1990).
[3] S. Maripuu, Nucl. Phys. **A149**, 593 (1970).
[4] I. Fodor, J. Sziklai, P. Kleinwächter, H. Schobbert, and F. Herrmann, J. Phys. G **5**, 1267 (1979).
[5] P. Kleinwächter, H. U. Gersch, and H. Schobbert, Nucl. Phys. **A398**, 476 (1983).
[6] J. Sziklai, J. A. Cameron, and I. M. Szöghy, in *Capture Gamma-Ray Spectrosopy and Related Topics (Holiday Inn–World's Fair, Knoxville, Tennessee)*, Proceedings of the Fifth International Symposium on Capture Gamma-ray Spectroscopy and Related Topics, AIP Conf. Proc. No. 125, edited by S. Raman (AIP, New York, 1985), p. 688; McMaster Accelerator Annual report 1986, p. 13.
[7] I. A. Al-Agil, G. U. Din, A. M. A. Al-Soraya, S. A. Baghazi, and J. A. Cameron, Phys. Rev. C **42**, 530 (1990).
[8] S. Galès, S. Fortier, H. Laurent, J. M. Maison, and J. P. Schapira, Phys. Rev. C **14**, 842 (1976).
[9] J. D. Moses, H. W. Newson, E. G. Bilpuch, and G. E. Mitchell, Nucl. Phys. **A175**, 556 (1971).
[10] W. R. Wylie, F. Zamboni, and W. Zych, Helv. Phys. Acta **44**, 757 (1971).
[11] Y. Ozawa, Y, Oguri, and E. Arai, Nucl. Phys. **A440**, 13 (1985).
[12] G. U. Din, A. M. Al-Soroya, J. A. Cameron, and J. Sziklai, Phys. Rev. C **31**, 1566 (1985).
[13] P. H. Vuister, Nucl. Phys. **83**, 593 (1966).
[14] G. U. Din, J. A. Cameron, V. P. Janzen, and R. B. Schubank, Phys. Rev. C **31**, 800 (1985).
[15] G. U. Din and J. A. Cameron, Phys. Rev. C **38**, 633 (1988).
[16] G. U. Din and J. A. Cameron, Phys. Rev. C **40**, 577 (1989).